Support Informating

Europium(III) complex-functionalized mangetic nanoparticle as a chemosensor for ultrasensitive detection and removal of copper (II) from aqueous solution

Jing Liu,[a] Wei Zuo,[a] Wei Zhang,[b] JianLiu,[a] Zhiyi Wang,[a] Zhengyin Yang,[a] Baodui Wang ,*[a]

[a]Key Laboratory of Nonferrous Metal Chemistry and Resources Utilization of Gansu Province and State Key Laboratory of Applied Organic Chemistry Lanzhou University Gansu, Lanzhou, 730000 (P.R. China) Lanzhou University, Lanzhou 730000, P.R. China.

[b]Key Laboratory of Preclinical Study for New Drugs of Gansu Province, School of Basic Medical Sciences, Lanzhou University, Lanzhou 730000, P.R. China.

E-mail: wangbd@lzu.edu.cn

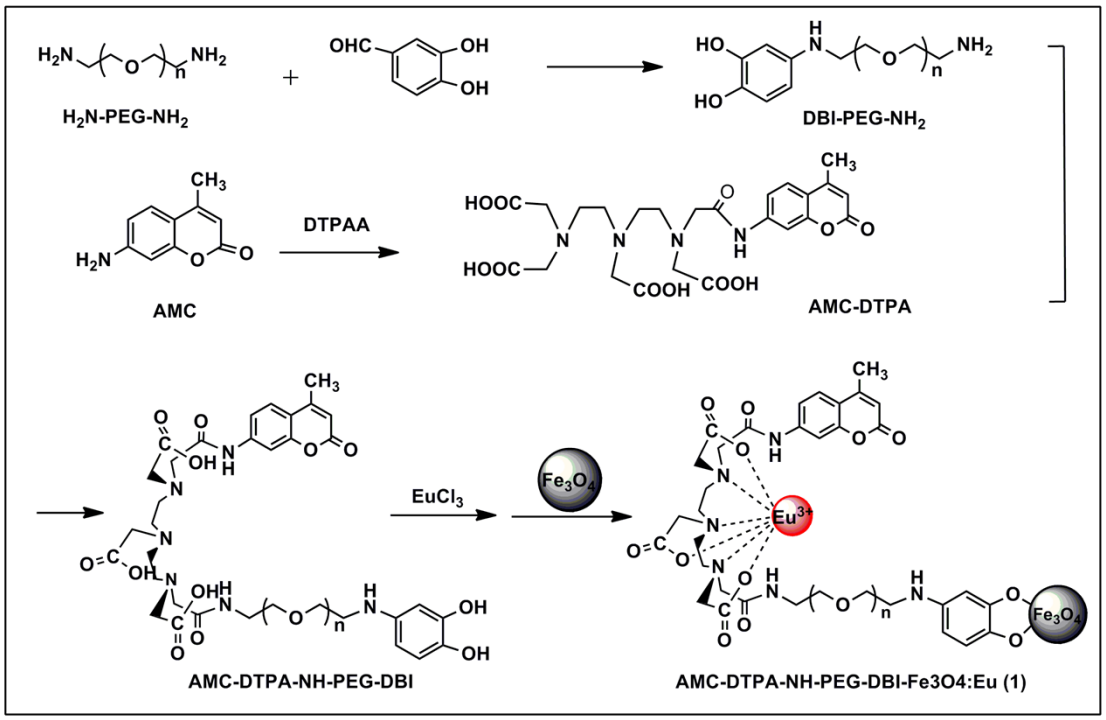

Scheme S1. Synthesis of Fe_3O_4-DBA-PEG-NH-DTPA-AMC:Eu^{3+} (**1**)

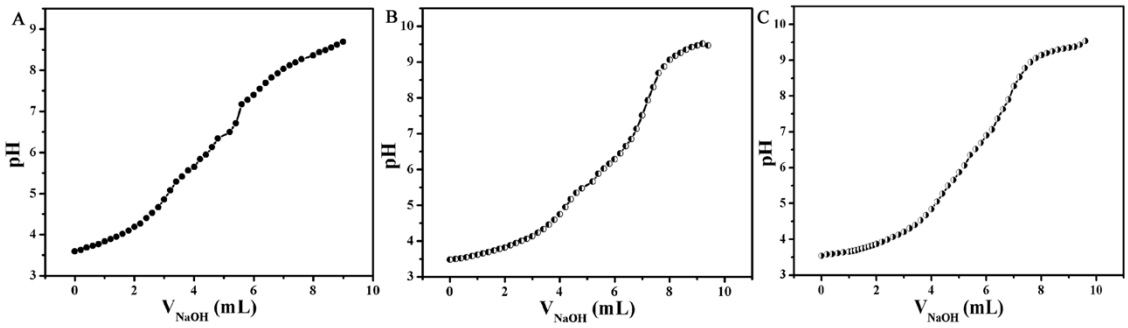

Figure S1. Potentiometric titration V-pH curves for the DTPA-AMC (A), Eu:DTPA-AMC complex (B) and Cu:DTPA-AMC complex (C) system at 25 °C and I = 0.1 mol dm^{-3} NaCl.

$$\bar{n}_H = \frac{jC_L + C_A + [OH^-] - [Na^+] - [H^+]}{C_L} \quad (1)$$

$$\bar{n}_H = \frac{\beta_1^H [H^+] + 2\beta_2^H [H^+]^2 + \ldots + j\beta_j^H [H^+]^j}{1 + \beta_1^H [H^+] + \beta_2^H [H^+]^2 + \ldots + \beta_j^H [H^+]^j} \quad (2)$$

$$[L] = \frac{jC_L + C_A + [OH^-] - [Na^+] - [H^+]}{\beta_1^H [H^+] + 2\beta_2^H [H^+]^2 + \ldots + j\beta_j^H [H^+]^j} \quad (3)$$

$$\bar{n} = \frac{C_L - \dfrac{jC_L + C_A + [OH^-] - [Na^+] - [H^+]}{\bar{n}_H}}{C_M} \quad (4)$$

Where j is the amount of H^+ in ligand acid H_jL, C_L is the concentration of H_jL, C_A is the concentration of strong acid, $[H^+]$ is obtained from pH value measured, $[OH^-]$ is obtained from the water constant of $K_W=[H^+][OH^-]$ at experimental temperature and $[Na^+]$ is the concentration of NaOH in solution, β_1^H, β_2^H, β_j^H are the cumulative protonation constants and C_M is the concentration of metal ion analyzed.

According the Bjerrun's Half-$\bar{n}$ Method and the data of Figure S1A, the values of pH and $\bar{n}_H$ computed by the equation (1) were analyzed to calculate the protonation constant of ligand. The protonation constant of ligand DTPA-AMC was presented as Table S1.

Table S1. The protonation constant of ligand.

Ligand	K_1^H	K_2^H	K_3^H	K_4^H
DTPA-AMC	$10^{6.42}$	$10^{5.01}$	$10^{4.14}$	$10^{3.81}$

According the Bjerrun's Half-$\bar{n}$ Method and the data of Figure S1B and Figure S1C, the values of pL and $\bar{n}$ computed by the equation (2)-(4) were analyzed to calculate the stability constant of complex. The stability constants of complexes Eu:DTPA-AMC and Cu:DTPA-AMC were presented as Table S2.

Table S2. The stability constants of complexes.

Complex	K_1	K_2	K_3	K_4	K
Eu:DTPA-AMC	$10^{3.91}$	$10^{4.29}$	$10^{5.52}$	$10^{5.95}$	$10^{19.67}$
Cu:DTPA-AMC	$10^{3.96}$	$10^{4.43}$	$10^{6.43}$	$10^{6.95}$	$10^{21.77}$

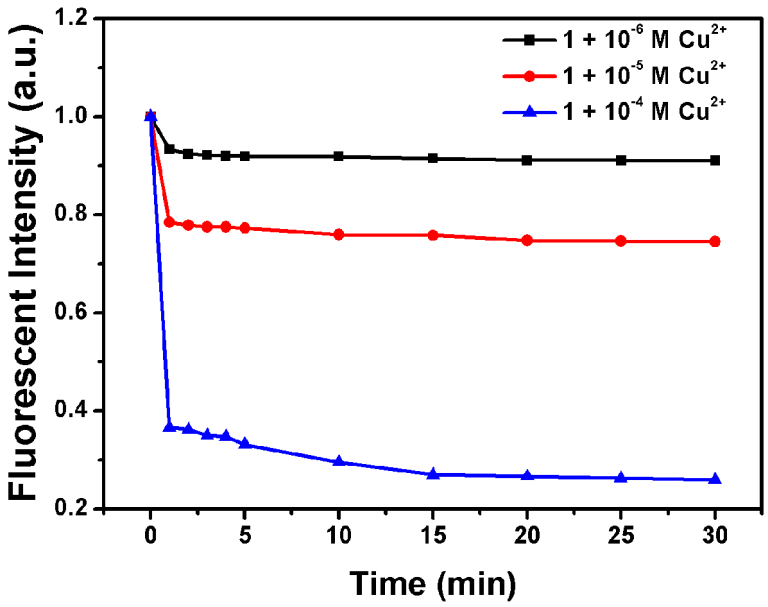

Figure S2. Reaction times on the emission intensity of 10 μM **1** with 1 μM, 10 μM and 100 μM Cu^{2+} in Tris-HCl buffer (50 mM, pH 7.20) at

616 nm, respectively.

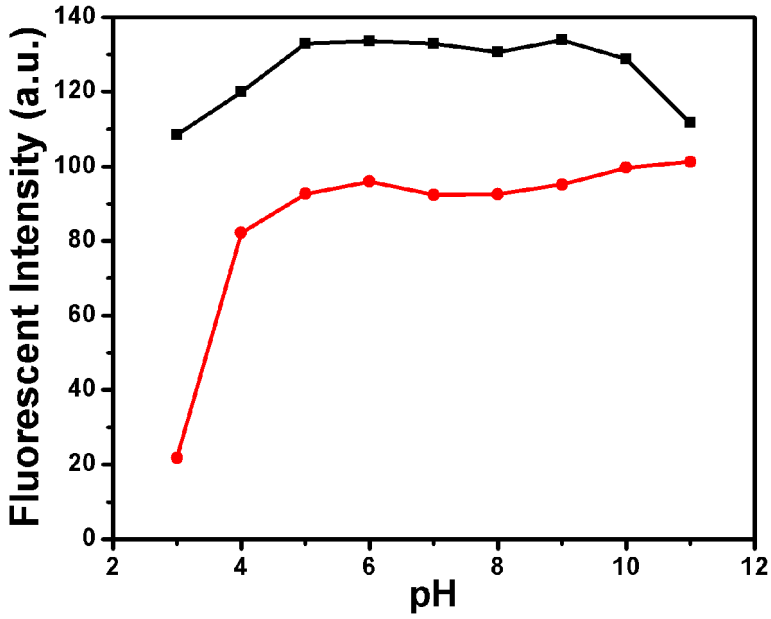

Figure S3. Effects of pH value on the emission intensity of 10 μM **1** without Cu^{2+} (black) and with 10 μM Cu^{2+} (red) in Tris-HCl buffer (50 mM, pH 7.20) at 616 nm.

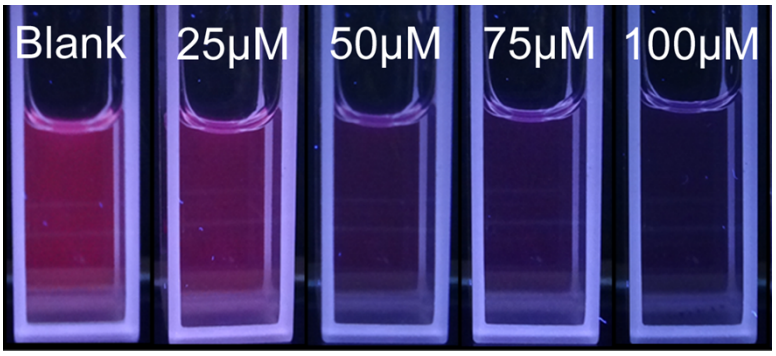

Figure S4. From left to right are fluorescence photographs of 10μM **1** after addition of 0 μM, 25 μM, 50 μM, 75 μM, 100 μM Cu^{2+} under UV light (254 nm) in Tris-HCl buffer(50 mM, pH 7.20).

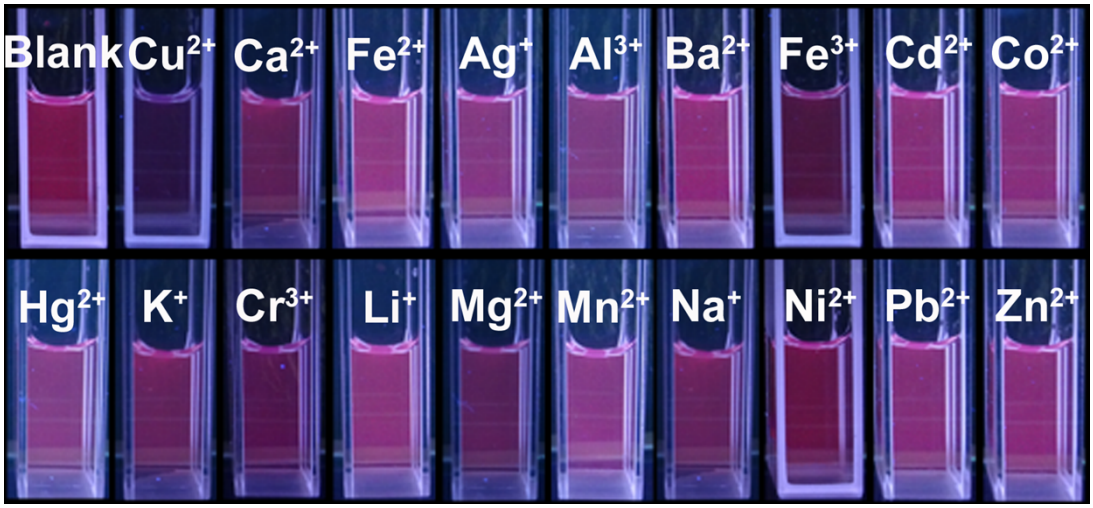

Figure S5. Fluorescence photographs changes of 10 μM **1** in the presence of 50 μM metal ions under UV light (254 nm) in Tris-HCl buffer (50 mM, pH 7.20).

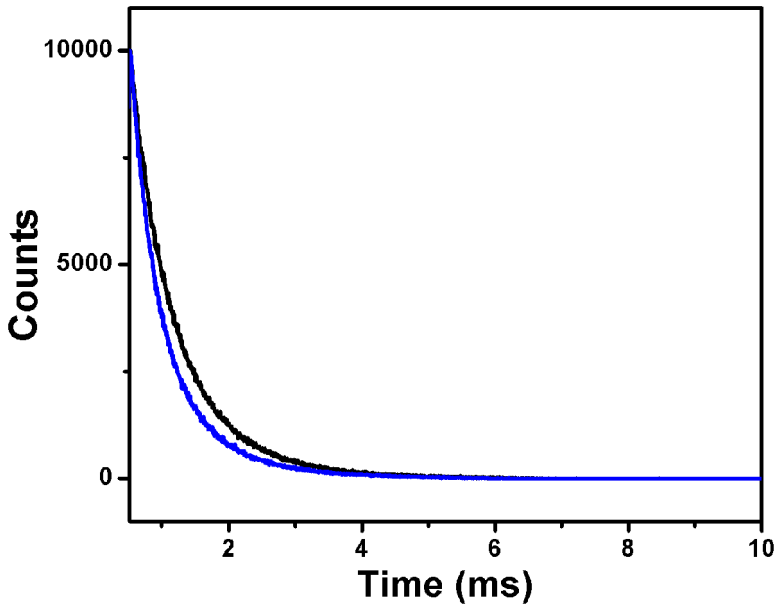

Figure S6. Fluorescent emission decay curves of 50 μM **1** without (black) and with 7 μM Cu^{2+} (blue) at 616 nm.

Table S3. Fluorescent lifetimes of **1** before and after addition of Cu^{2+}.

Samples	τ_1 (ms)	Relative weighting (%)	τ_2 (ms)	Relative weighting (%)	$<\tau>^a$ (ms)
1	0.56	56	1.16	44	0.83
1 + 7μM Cu^{2+}	0.41	51	1.06	49	0.73

[a]Averaged lifetimes was calculated using the equation $<\tau>=\sum A_i\tau_i^2 / \sum A_i\tau_i$, where A_i are the preexponential factors related with the statistical weights of each exponential.

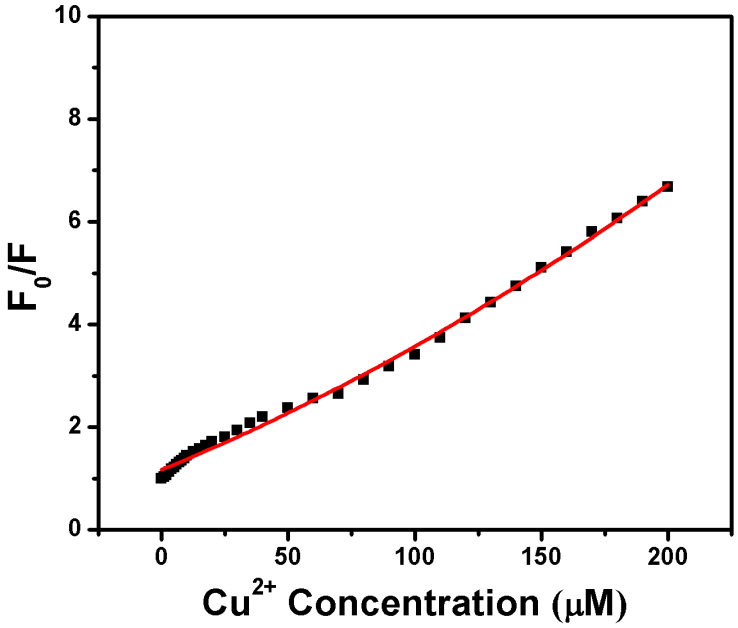

Figure S7. The Fluorescent intensity ratio F_0/F changes of 10 μM Fe_3O_4 NPs-Eu^{3+} complex in the presence of different concentration of Cu^{2+} at 616 nm. F_0 and F are the fluorescence intensities of **1** in the absence and presence of Cu^{2+}, respectively.

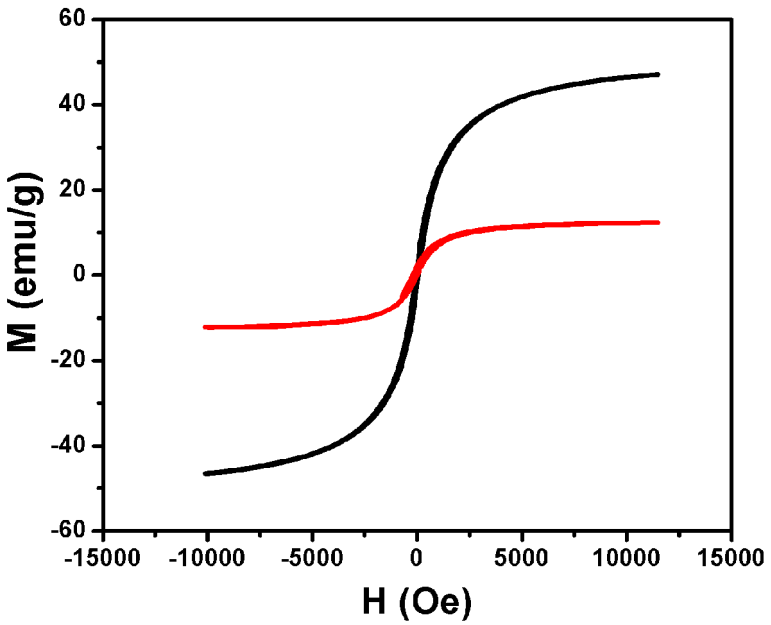

Figure S8. The magnetization hysteresis loops of Fe_3O_4 NPs (black) and **1**(red).

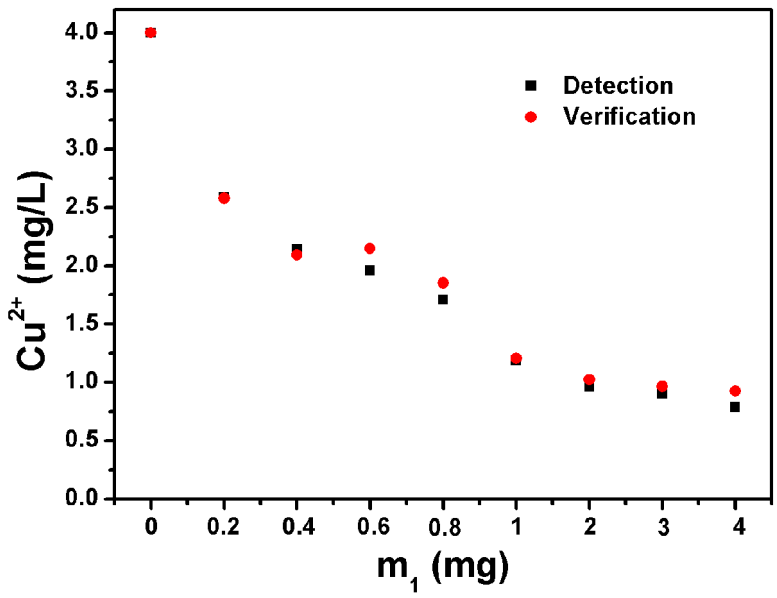

Figure S9. Detection and verification of the estimated Cu^{2+} concentration after magnetic separation.

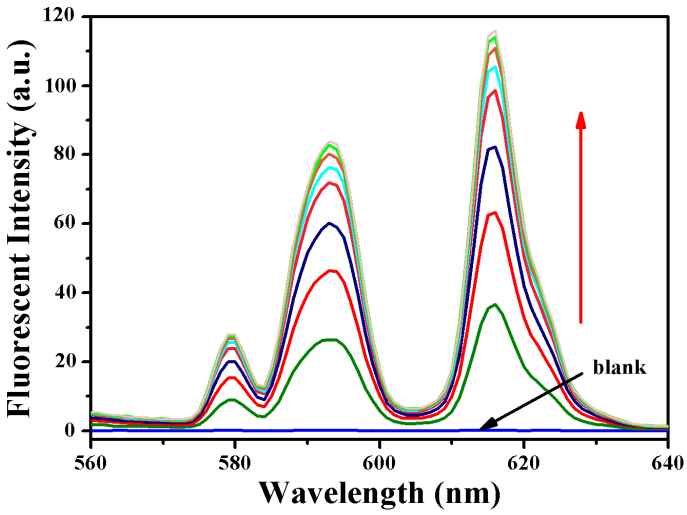

Figure S10. The fluorescent emission spetra of 10 μM Eu^{3+} in the presence of different concentration of Fe_3O_4-DBA-PEG-NH-DTPA-AMC (0, 0.1 mg/L, 0.2 mg/L, 0.3 mg/L, 0.4 mg/L, 0.5 mg/L, 0.6 mg/L, 0.7 mg/L, 0.8 mg/L).

Table S4. The Cu^{2+} concentration before and after separation by nanocomposite **1** and the verification of the estimated Cu^{2+} concentration after magnetic separation and the removal efficiency.

Nanocomposite **1** (mg)	0	0.2	0.4	0.6	0.8	1	2	3	4
$[Cu^{2+}]_{start}$ (ppm)	4	4	4	4	4	4	4	4	4
$[Cu^{2+}]_{final\ detect}$(ppm)	4	2.59	2.14	1.95	1.71	1.19	0.96	0.90	0.79
$[Cu^{2+}]_{final\ verification}$ (ppm)	4	2.58	2.09	2.15	1.85	1.21	1.02	0.97	0.92
Remove efficiency (%)	0	35	46	51	57	70	76	77	80